

## Combined DCE and DW-MRI in the diagnosis of benign and malignant tumors of the tongue

Songtao Ai<sup>1</sup>, Wenjing Zhu<sup>1</sup>, Yu Liu<sup>1</sup>, Pingzhong Wang<sup>1</sup>, Qiang Yu<sup>1</sup>, Kerong Dai<sup>2</sup>

<sup>1</sup>Department of Radiology, Shanghai Ninth People's Hospital, School of Medicine, Shanghai Jiao Tong University, Shanghai, China, <sup>2</sup>Engineering Research Center of Digital Medicine, Ministry of Education, Department of Orthopaedics, Ninth People's Hospital, Shanghai Jiao Tong University School of Medicine, Shanghai, China

### TABLE OF CONTENTS

1. Abstract
2. Introduction
3. Patients and methods
  - 3.1. Patients
  - 3.2. MRI examination
  - 3.3. MRI evaluation
  - 3.4. Statistical analysis
4. Results
  - 4.1. Patients
  - 4.2. MRI evaluation
  - 4.3. TIC pattern analysis derived from DCE-MRI
  - 4.4. Threshold values
  - 4.5. Diagnostic value
5. Discussion
6. Conclusion
7. Acknowledgements
8. Reference

## 1. ABSTRACT

The combination of dynamic contrast-enhanced (DCE) and diffusion-weighted (DW)-MRI adds important information to the findings obtained through conventional spin echo MRI. We aimed to determine the value of combined DW- and DCE-MRI in distinguishing benign from malignant tumors of the tongue and mouth floor. The apparent diffusion coefficient (ADC) maps were constructed, and the ADC values of the lesions were calculated from DW-MRI. The slopes were derived from time-intensity curves (TICs) from DCE-MRI. The ADC map for malignant tumors was lower compared with the benign lesions. The slope in the malignant tumors was significantly greater compared with the benign lesions. In malignant tumors, the ADC<sub>b=500</sub> threshold of  $<1.43 \times 10^{-3}$  mm<sup>2</sup>/s yielded a sensitivity, specificity, and accuracy of 74.6%, 83.3%, and 79.7%, respectively. For benign lesions, a slope threshold of  $<38.6$  yielded a sensitivity, specificity, and accuracy of 80.3%, 74.5%, and 77.9%, respectively. Combined DCE- and DW-MR imaging may provide valuable information that allows for the differentiation between benign lesions and malignant tumors of the tongue and mouth floor.

## 2. INTRODUCTION

The preoperative diagnosis of benign from malignant tumors of the tongue is critical for surgical planning because the treatment and prognosis differ significantly. Benign lesions generally include vascular malformations, inflammatory masses, cysts, and pleomorphic adenomas. Vascular malformations are treated with sclerotherapy, laser, catheter embolization, and direct puncture (1, 2, 3). Local excision with safety margins of a cyst mass or adenoma is performed to treat these benign lesions (4, 5). In contrast, treatment of malignant tongue carcinoma generally involves surgery in combination with radiotherapy. Surgical treatment of tongue carcinoma requires extensive resection of the oropharynx, which causes significant functional deficits (6, 7). The pathological biopsy is a minimally invasive procedure used for the preoperative diagnosis of a tongue tumor. However, insufficient biopsy specimens are sometimes obtained, and the results derived are not always conclusive (8). Moreover, the diagnostic accuracy of intraoperative frozen section analysis is significantly superior to preoperative biopsy (8). Therefore, preoperative imaging plays an important role in the treatment selection and surgical planning.

Recently, static magnetic resonance imaging (MRI) has been used extensively for the diagnosis of tumors in the oral and maxillofacial region. In static MR images, malignant tumors are characterized by an irregular tumor margin, signal intensity heterogeneity, infiltration into surrounding tissue, and low signal intensity on T<sub>2</sub>-weighted images. For example, Som and Biller (9) reported that malignant parotid tumors were commonly associated with poorly defined margins and low signal intensity in T<sub>1</sub>- and T<sub>2</sub>-weighted images. Conversely, Freling reported that tumor margin, homogeneity, and signal intensity were not discriminative factors that correctly distinguished benign from malignant disease (10). Teresi reported that tumor homogeneity was not a useful criterion to distinguish benign from malignant disease (11). The malignant tumors exhibited deep structure infiltration, whereas infiltration into the subcutaneous fat was observed in inflammatory diseases and malignancies (10, 12). Therefore, the role of static MR imaging in the differentiation of benign lesions from malignant tumors is controversial.

Malignant tumors rely not only on passive diffusion from host blood vessels but also on newly developed vasculature (angiogenesis) to proliferate. Moreover, vessels produced by angiogenesis associated with malignancies are leaky, fragile, and incompletely formed. Dynamic contrast-enhanced (DCE)-MRI is an imaging modality that reflects the density, integrity, and leakiness of the tumor vasculature. The parameters calculated from DCE-MRI are used to assess the histological properties of the tumor (13). Therefore, many investigators have attempted to identify the difference between benign lesions and malignant tumors, as well as assess the malignant potential of these tumors using DCE-MRI (14, 15, 16, 17, 18). Diffusion-weighted (DW)-MRI is based on the random thermal motion of water molecules termed Brownian motion. The differences in the translational diffusion of water molecules are quantified using apparent diffusion coefficients (ADCs) (19). ADCs vary according to the tissue's microstructure or pathophysiological state and are inversely correlated to tissue cellularity (19). Malignant tumors are associated with alterations in the cellularity, cellular and nuclear contour, and extracellular matrix. The use of DW-MRI to distinguish benign lesions from malignant tumors or grade malignancies has been reported in prior studies (20, 21, 22, 23, 24, 25, 26, 27).

DCE-MRI provides hemodynamic information not available with conventional MRI and could be potentially applied to differentiate benign lesions from malignant tumors. However, it provides no information on cellularity, mitosis, or atypia specific to tumor cells, which are important determinants for tumor categorization. In contrast, DW-MRI reveals tumor cellularity, mitosis, and nuclear contour differences in the molecular translational motion of water. We postulated that the combination of DCE- and DW-MRI compensates for the disadvantages of each separate technique and thereby adds important information to the findings obtained through conventional spin echo MRI. The purpose of the study is to investigate the diagnostic value of combined DCE- and DW-MRI in distinguishing benign lesions from malignant tongue tumors. The ADC map, ADC value, slope, and TIC obtained from the MRI studies were examined.

### **3. PATIENTS AND METHODS**

#### **3.1. Patients**

This retrospective study was approved by the hospital's review committee, and written informed consent was obtained from all of the patients. A total of 79 consecutive patients were examined from January 2005 to June 2007 at our hospital using MRI and diagnosed with tumors of the tongue. All patients then underwent DCE-MRI and DW-MRI at our hospital. Thirty-three patients were excluded due to a tumor diameter <15 mm according to the MRI results (7), obscure tumor margins on DW-MRI (12), an obvious susceptibility artifact from a denture or metal implant within the oral cavity (8), or a significant motion artifact (6). The remaining 46 patients were enrolled in this study. The final diagnoses were based on the pathological findings in the specimens obtained at surgical resection. This study followed the Declaration of Helsinki on medical protocol and ethics, and the regional Ethical Review Board of Shanghai Ninth People's Hospital (Shanghai, China) approved the study.

#### **3.2. MRI examination**

MRI examinations were performed prior to surgery in all 46 patients using a 1.5 Tesla MR scanner (Signa MR/i, GE Medical System, Milwaukee, WI, USA) with head and neck array coils. All MRI, DW-MRI, and DCE-MRI examinations consisted of a 5-mm section thickness and a 1-mm intersection gap, 228 × 192 acquisition matrix, and 24 × 18 cm field of view (FOV). Transverse T1-weighted spin echo (SE) sequences were performed with a repetition time (TR) of 400 ms and an echo time (TE) of 8 ms. Transverse T2-weighted fast spin echo (FSE) sequences were performed with a TR of 4,020 ms and TE of 84.8 ms.

DW-MRI examinations were performed using a SE single shot echo-planar imaging (EPI) sequence in the transverse plane with a TR of 4,000 ms and TE of 51.8 ms. Sensitizing diffusion gradients were applied sequentially in the x, y, and z direction with b-values set at 500 or 1,000 s/mm<sup>2</sup>. ADC maps were generated. Tongue tumors were identified on the transverse T1-weighted MR images, and three sections (one section accounted for the maximum diameter of the tumor) were selected for DCE imaging. FSE T1-weighted images were obtained with a TR of 400-600 ms and a TE of 8-9.9 ms. Gadolinium diethylenetriamine pentaacetic acid (Gd-DTPA, Magnevist, Schering, Berlin, Germany) was administered intravenously at a rate of 2 mL/s (total dose, 0.1 mmole per kg of body weight) using a power injector, followed by a 20 mL saline flush. DCE images were sequentially obtained prior to and at 0, 30, 60, 90, 120, 150, 180, 210, 240, 270, and 300 s following administration of contrast material. The total acquisition time was approximately 8 minutes.

#### **3.3. MRI evaluation**

All MR images were interpreted and consensus was achieved by two radiologists (14 and 15 years of experience in head and neck MR imaging, respectively) who were blinded to clinical information and the

**Table 1.** ADC or slope value among histopathologic diagnoses

Diagnosis	Group	ADC (b value = 500 s/mm <sup>2</sup> ; mm <sup>2</sup> /s)	Slope
Benign lesions (n = 13)	Vascular Malformations (n = 11)	1.66 ± 0.43 × 10 <sup>-3</sup>	38.53 ± 5.48
	Cyst (n = 1)	3.53 × 10 <sup>-3</sup>	57.80
	Pleomorphic Adenoma (n = 1)	1.22 × 10 <sup>-3</sup>	35.72
Malignant tumor (n = 33)	Squamous Cell Carcinoma (n = 28)	1.22 ± 0.27 × 10 <sup>-3</sup>	41.03 ± 12.5
	Adenoid Cystic Carcinoma (n = 2)	1.04 ± 0.24 × 10 <sup>-3</sup>	54.97 ± 20.0
	Non-Hodgkin's Lymphoma (n = 2)	0.93 ± 0.39 × 10 <sup>-3</sup>	41.72 ± 4.30
	Mucoepidermoid Carcinoma (n = 1)	1.72 × 10 <sup>-3</sup>	46.29

histopathologic results. The regions of interest (ROIs) were manually drawn for measurements of signal intensity to avoid the vessels and cystic regions of the tumor tissue. For cases in which the contrast enhancement was heterogeneous, the signal intensity (SI) of multiple areas was measured, and the area with maximal enhancement was selected. Thereafter, we plotted the average signal intensity within the ROI against time and constructed time-intensity curves (TICs). The slope value was derived from the TICs. The SI<sub>peak</sub> was defined as the first SI measurement that satisfied the inequality SI > (0.9 (SI<sub>max</sub> - SI<sub>pre</sub>)) + SI<sub>pre</sub>. The T<sub>peak</sub> represented the time that corresponded with the SI<sub>peak</sub>. The SI<sub>pre</sub> represented the pre-contrast signal intensity, and the SI<sub>max</sub> was defined as the signal intensity at maximal contrast enhancement. We did not define the T<sub>peak</sub> as the time that corresponded with the SI<sub>max</sub>. In previous investigations, we defined the T<sub>peak</sub> as the time corresponding with the SI<sub>max</sub> and found it difficult to determine a reliable T<sub>peak</sub> value for cases in which the TIC exhibited an early peak and plateau enhancement pattern because the signal intensity changed only very slightly within a margin of error during the plateau phase. The slope was defined as follows: ((SI<sub>max</sub> - SI<sub>pre</sub>) / (SI<sub>pre</sub> × T<sub>peak</sub>)) × 100.

To obtain the ADC measurement, the same radiologists manually identified ROIs within a given lesion. Three ROIs were placed within the area that corresponded to the area used for TIC construction, and we obtained the average ADC values of the 3 ROIs. We also chose ROIs in which obvious cystic areas could be avoided for TIC construction and ADC measurements. Pixel-based ADC maps were obtained from a commercial workstation. ADCs were calculated using linear regression analysis of the function ln(S/S0) = -b × ADC, where S represents the SI after application of the diffusion gradient, S0 represents SI with a b-value of 0 s/mm<sup>2</sup>, and b is the b-value.

**3.4. Statistical analysis**

Statistical analyses were performed using the SPSS 10.0 statistical software package (SPSS, Chicago, IL, USA: 1999). Numeric data were reported as means ± standard deviation. The unpaired t-test was used to compare the TIC parameters and ADCs of benign lesions with those of malignant tumors. The chi-squared (χ<sup>2</sup>) test was used to compare the TIC patterns between benign lesions and malignant tumors. Using SPSS and receiver operating characteristic (ROC) curve analysis of the slope and ADC, the diagnostic ability to differentiate between benign and malignant conditions was evaluated. The specificity, sensitivity, accuracy, positive predictive value (PPV), and negative predictive value (NPV) were calculated based on the corresponding threshold value. A

probability (P)-value < 0.05 indicated a significant difference.

**4. RESULTS**

**4.1. Patients**

Thirteen patients (age range: 7-69 years; mean age: 35.00 ± 18.27 years; male/female ratio: 7/6) had benign lesions that consisted of eleven cases of vascular malformation, one cyst, and one pleomorphic adenoma. There were 33 patients with malignant tumors (age range: 26-84 years; mean age: 55.33 ± 15.69 years; male/female ratio: 23/10), including 28 squamous cell carcinomas (SCCs), 2 adenoid cystic carcinomas (ACCs), 2 non-Hodgkin's lymphomas (NHLs), and one mucoepidermoid carcinoma.

**4.2. MRI evaluation**

Table 1 displays the mean ADC or slope values among various histological diagnoses. Figure 1A shows the distribution of ADC values. The mean ADC value for malignant tongue tumors was (1.21 ± 0.29) × 10<sup>-3</sup> mm<sup>2</sup>/s and was significantly less compared with benign lesions [(1.69 ± 0.67) × 10<sup>-3</sup> mm<sup>2</sup>/s at the b-value 500 s/mm<sup>2</sup>] (P = 0.00122). Figure 1B shows the distribution of slope values. The mean slope value for the malignant tumors (46.08 ± 10.40) was significantly greater compared with benign lesions (38.10 ± 7.74; P = 0.001201). Thus, both the ADC and slope measurements were useful in distinguishing benign lesions from malignant tongue tumors.

**4.3. TIC pattern analysis derived from DCE-MRI**

Based on the T<sub>peak</sub> and enhancement patterns, the tongue tumors were categorized into three TIC patterns. Type I represents a T<sub>peak</sub> <90 s, a rapid enhancement, and a persistent plateau. Type II reflects a T<sub>peak</sub> >90 s and an enhancement that increases relatively rapidly. A Type III TIC exhibits a gradual enhancement over three minutes. Table 2 shows the distribution of benign lesions and malignant tumors among the three TIC classifications. In all 13 benign lesions, only one (8%) vascular malformation was considered to be a type I; the remaining were considered to be type II or III. Of the 33 malignant tumors, 22 SCCs (67%), 2 ACCs (6%), 2 NHLs (6%), and one mucoepidermoid carcinoma (3%) were considered to be type I; only 5 SCCs (15%) were considered type II, and one SCC (3%) was considered type III. The χ<sup>2</sup> value was 22.121, and the P-value was 0.000 for the distribution of the TIC pattern. These findings clearly indicate that TIC patterns are useful when differentiating between benign lesions and malignant tongue tumors.

**Table 2.** TIC patterns among histopathologic diagnoses

Diagnosis	Group	TIC Pattern		
		A	B	C
Benign lesions (n = 13)	Vascular Malformations (n = 11)	1	4	2
	Cyst (n = 1)			1
	Pleomorphic Adenoma		1	
Malignant tumors (n = 33)	Squamous Cell Carcinoma (n = 28)	22	5	1
	Adenoid Cystic Carcinoma (n = 2)	2		
	Non-Hodgkin's Lymphoma (n = 2)	2		
	Mucoepidermoid Carcinoma (n=1)	1		

TIC:time-intensity curves

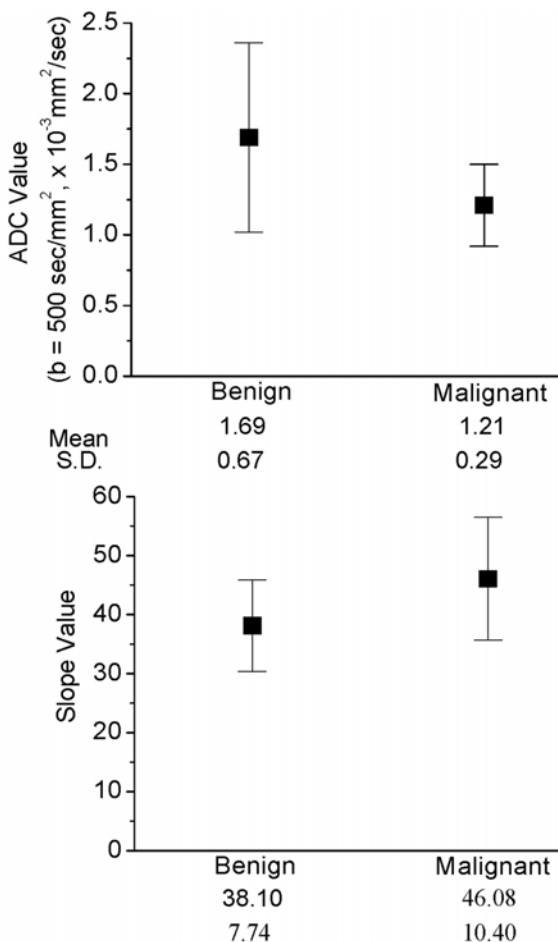


**Figure 1.** The mean ADC and slope values (vertical axis) of benign or malignant tongue tumors. The mean ADC values in benign and malignant tumors are  $(1.69 \pm 0.67) \times 10^{-3} \text{ mm}^2/\text{s}$  and  $(1.21 \pm 0.29) \times 10^{-3} \text{ mm}^2/\text{s}$ , respectively (A). The mean slope values for benign and malignant tumors are  $38.1 \pm 7.74$  and  $46.08 \pm 10.40$ , respectively (B). The order of A to B is from left to right.

**4.4. Threshold values**

The ROC-based positive test was performed to produce reasonable threshold values. To distinguish benign lesions from malignant tongue tumors, the ADC threshold value was  $1.43 \times 10^{-3} \text{ mm}^2/\text{s}$  and the slope threshold value was 38.6.

**4.5. Diagnostic value**

Table 3 summarizes the performance values based on the ADC and slope thresholds. With an ADC

threshold of  $1.43 \times 10^{-3} \text{ mm}^2/\text{s}$ , the sensitivity, specificity, accuracy, PPV, and NPV were 74.6%, 83.3%, 79.7%, 89.9%, and 59.4%, respectively. When an ADC threshold of 38.6 was applied, the sensitivity, specificity, accuracy, PPV, and NPV were 80.3%, 74.5%, 77.9%, 89.2%, and 60.1%, respectively.

Figure 2-11 shows two representative cases in which the ADC and slope thresholds were both used to assign the correct diagnosis. The malignant SCC (Figure 2, 3) exhibited an ADC value of  $1.09 \times 10^{-3} \text{ mm}^2/\text{s}$  (less than the threshold value of  $1.43 \times 10^{-3} \text{ mm}^2/\text{s}$ ) and a slope value of 48.7 (greater than the threshold value of 38.6). The benign vascular malformation (Figure 6, 7) had an ADC value of  $2.45 \times 10^{-3} \text{ mm}^2/\text{s}$  (greater than the threshold value of  $1.43 \times 10^{-3} \text{ mm}^2/\text{s}$ ) and slope value of 33.2 (less than the threshold value of 38.6) (Figure 4, 5). In these cases, both the DCE-MRI and DW-MRI were independently useful for differentiating benign lesions from malignant tongue tumors.

There were exceptions where a diagnosis was made incorrectly according to either DCE- or DW-MRI alone. Figure 6-11 shows three representative cases where we used a combination of DCE-MRI and DW-MRI to rectify the diagnosis. In Figures 6 and 7, the TIC of a benign cyst exhibited an enhancement peak, followed by a completely washed-out pattern. Moreover, the slope of the cyst (57.8) was significantly higher than the threshold value (38.6). Therefore, the cyst was misdiagnosed as malignant by DCE-MRI. Referring to the ADC value rectified the diagnosis because the ADC of the cyst ( $3.53 \times 10^{-3} \text{ mm}^2/\text{s}$ ) was substantially higher than the threshold value ( $1.43 \times 10^{-3} \text{ mm}^2/\text{s}$ ). Figures 8 and 9 show a benign pleomorphic adenoma that was misdiagnosed as malignant according to the ADC value of  $1.22 \times 10^{-3} \text{ mm}^2/\text{s}$ , which was less than the threshold value of  $1.43 \times 10^{-3} \text{ mm}^2/\text{s}$ . However, considering the slope value in addition to the ADC value correctly modified the diagnosis (35.72, which was less than the threshold value of 38.6). Figures 10 and 11 show that a malignant mucoepidermoid carcinoma was falsely considered a benign lesion based on the ADC value of  $1.72 \times 10^{-3} \text{ mm}^2/\text{s}$ , which was greater than the threshold value of  $1.43 \times 10^{-3} \text{ mm}^2/\text{s}$ . However, the diagnosis was rectified by considering the slope (46.29, which was greater than the threshold value of 38.6). Therefore, the combination of DCE-MRI and DW-MRI improved the diagnostic accuracy in differentiating benign lesions from malignant tongue tumors.

**5. DISCUSSION**

The preoperative diagnosis of benign lesions versus malignant tumors of the tongue is critical for surgical planning and treatment selection. The differential diagnosis of benign and malignant tumors of the tongue

Combined DCE- and DW-MRI in the diagnosis of the tongue tumors

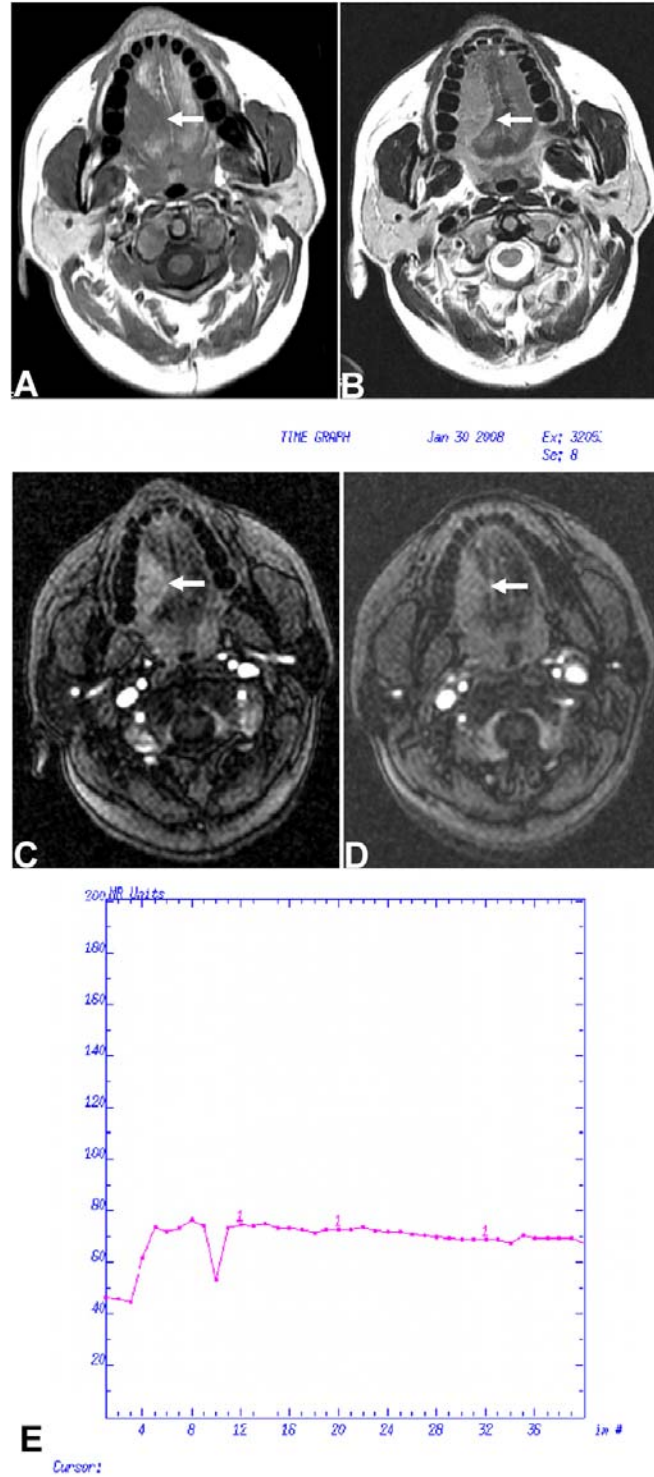


**Figure 2.** Squamous cell carcinoma of the right tongue in a 73-year-old man analyzed by DCE-MRI. (A) Transverse T1-weighted SE MR image shows a heterogeneously hyperintense mass (arrowhead) in the tongue dorsum. (B) Transverse T2-weighted FSE MR image shows a homogeneously hyperintense mass (arrowhead). (C) Transverse T1-weighted SE MR image obtained 30 s after contrast material administration shows early rapid wash-in (arrowhead). (D) Transverse T1-weighted SE MR image acquired 228 s after contrast material administration shows a delayed enhancement pattern (arrowhead). (E) TIC shows a rapid wash-in followed by plateau enhancement. The slope value is 48.7, which is substantially larger than the threshold value (38.6). The DCE-MRI is useful for the characterization of tongue tumors based on TIC analysis. The order of A to E is from left to right.

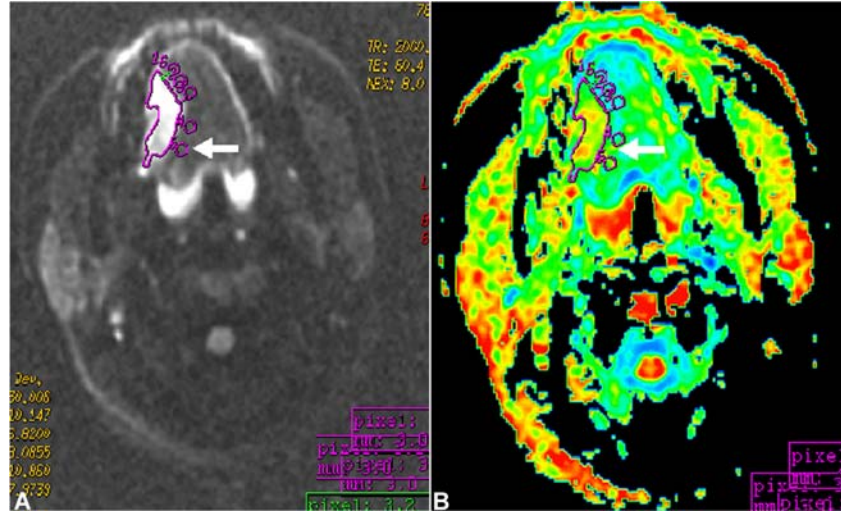


**Figure 3.** Squamous cell carcinoma of the right tongue in a 73-year-old man analyzed by DW-MRI. (A) Transverse diffusion-weighted MR image (b-value = 500 s/mm<sup>2</sup>) shows a homogeneously hyperintense mass (arrowhead). (B) ADC map shows a high-SI mass. The ADC value is 1.09×10<sup>-3</sup> mm<sup>2</sup>/s, which is significantly greater than the threshold value (1.43×10<sup>-3</sup> mm<sup>2</sup>/s). The DW-MRI is useful for the characterization of tongue tumors based on ADC measurements. The order of A to B is from left to right.

seems to be difficult using conventional static MRI. DCE-MRI reflects hemodynamic information not available with static MRI and has the potential to differentiate benign from malignant tumors. DW-MRI reveals tumor cellularity, mitosis, and nuclear contour-based differences in the molecular translational motion of water. The combination of DCE- and DW-MRI compensates for each technique's disadvantages and adds important information to conventional MRI. Therefore, we hypothesized that combined DCE- and DW- MRI examinations are valuable for distinguishing benign lesions from malignant tumors of tongue. This retrospective study was designed to test this hypothesis.

Our findings indicate that either DCE- or DW-MRI alone is valuable for predicting whether a tongue lesion is benign or malignant with a specificity of approximately 80% in this study.. Our results also indicate that there is a significant chance of misdiagnosis. Referring to the ADC values is particularly useful when differentiating benign lesions, which exhibit an increased slope value and malignant TIC pattern on DCE-MRI. Moreover, the additional analyses of TIC parameters taken from DCE-MRI results are extremely valuable for distinguishing a benign lesion with a low ADC value or a malignant tumor with a high ADC value. Therefore, the combination of DCE-MRI and DW-MRI potentially improves diagnostic specificity and accuracy in the characterization of tongue tumors.

The DCE-MRI results demonstrated that the mean slope of benign lesion was significantly less steep than the slope of malignant tumors. Most malignant tumors exhibited a type I TIC pattern, which is characterized by rapid enhancement until the SI<sub>max</sub> was reached followed by a persistent plateau. In comparison, the TIC results of most benign lesions were consistent with type II or III patterns,

exhibiting a gradual increase in enhancement over time. Thus, DCE-MRI parameters and TIC patterns are useful for differentiating between benign lesions and malignant tongue tumors.

The diagnostic value of TIC parameters and patterns observed in this study is in concordance with other investigations. Asaumi *et al.* (14) found that the maximum contrast index (CI<sub>max</sub>), the time to reach the CI<sub>max</sub>, and TIC patterns were valuable for differentiating malignant lymphomas and SCCs. Hisatomi *et al.* (15) and Yabuuchi *et al.* (16) reported that DCE-MRI parameters and TIC patterns were useful in the differential diagnosis of salivary gland tumors based on the combined assessment of the T<sub>peak</sub> and CI<sub>max</sub> or the washout ratio (WR). The findings indicated that a T<sub>peak</sub> of 120 s allowed for the differentiation of a malignant carcinoma from a benign pleomorphic adenoma but not from a Warthin's tumor. However, a WR of 30% enabled the differentiation between a malignant tumor and a Warthin's tumor (15, 16).

DCE-MRI patterns are affected by a wide range of pathophysiologic factors that include microvessel density, blood flow, endothelial permeability, cellularity-stromal grade, and the availability of an extracellular compartment (13). Microvessel density and blood flow are closely related to the T<sub>peak</sub>, CI<sub>max</sub>, and slope (16). The endothelial permeability, cellularity-stromal grade, and the availability of an extracellular compartment correlate with the WR. The extracellular compartment with fibrous stromata retains contrast agents for a longer time period (16, 28). Therefore, malignant tumors are generally associated with increased microvessel density, high vascularity, and cellularity. Therefore, malignant tumors exhibit rapid wash-in and a substantial enhancement and persistent plateau on MCE-MRI. However, in our study we found that one benign cyst was improperly diagnosed as malignant based

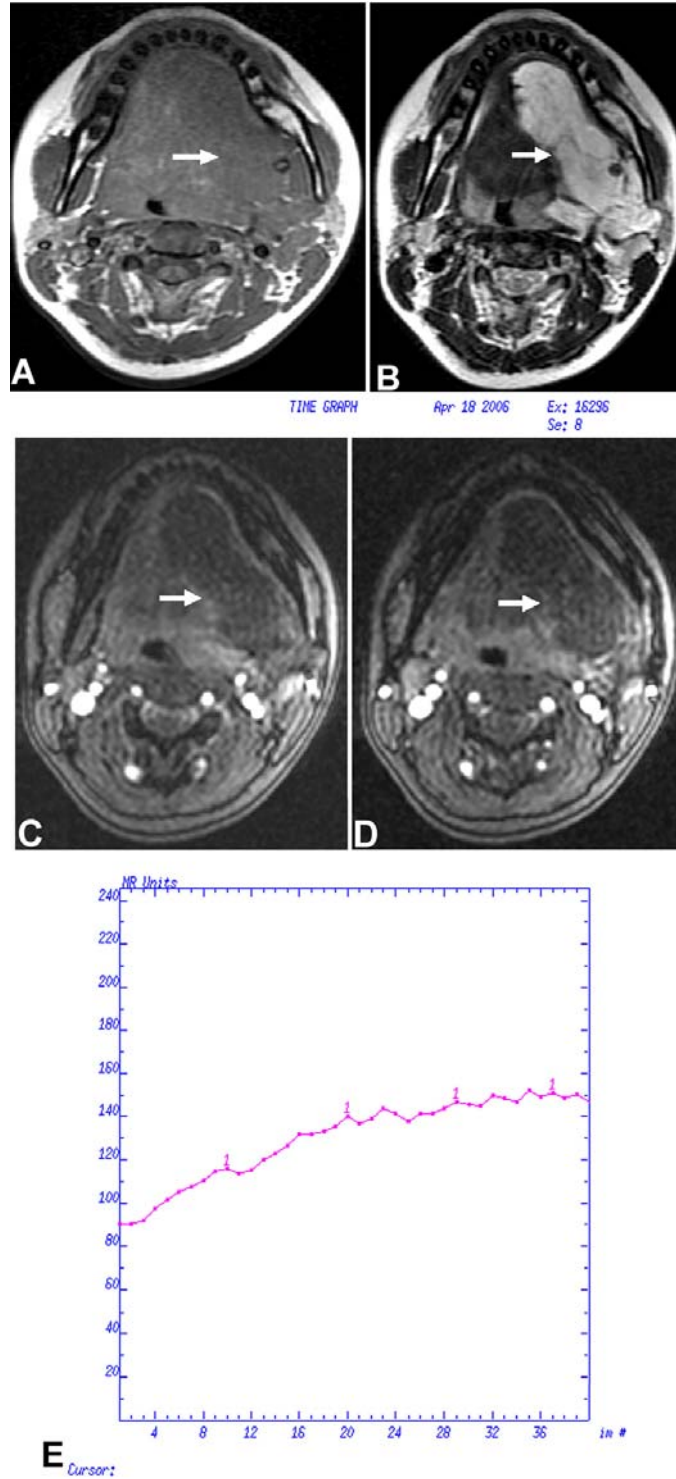


**Figure 4.** Vascular malformation of the left tongue in an 18-year-old woman analyzed by DCE-MRI. (A) Transverse T1-weighted SE MR image shows a non-intense mass (arrowhead) in the tongue dorsum. (B) Transverse T2-weighted FSE MR image shows a homogeneously hyperintense mass (arrowhead). (C) Transverse T1-weighted SE MR image obtained 30 s after contrast material administration shows early delayed wash-in (arrowhead). (D) Transverse T1-weighted SE MR image acquired 228 s after contrast material administration shows a delayed enhancement pattern (arrowhead). (E) TIC shows a slow and gradual enhancement. The slope value is 33.2, which is substantially smaller than the threshold value (38.6). The DCE-MRI is useful for the characterization of tongue tumors based on TIC analysis. The order of A to E is from left to right.



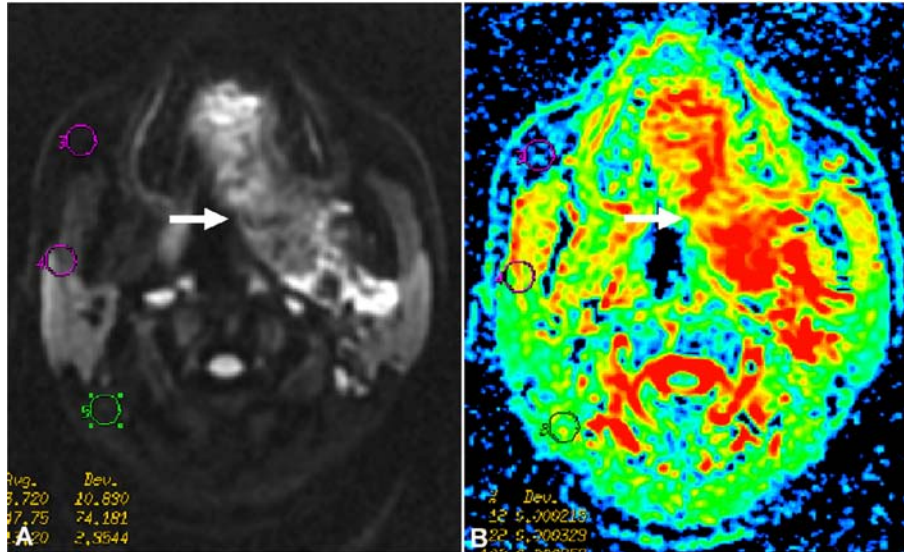


**Figure 5.** Vascular malformation of the left tongue in an 18-year-old woman analyzed by DW-MRI. (A) Transverse DW-MR image (b-value =  $500 \text{ s/mm}^2$ ) shows a heterogeneously hyperintense mass (arrowhead). (B) ADC map shows a low-SI mass. The ADC value is  $2.45 \times 10^{-3} \text{ mm}^2/\text{s}$ , which is significantly more than the threshold value ( $1.43 \times 10^{-3} \text{ mm}^2/\text{s}$ ). The DW-MRI is useful for the characterization of tongue tumors based on ADC measurements. The order of A to B is from left to right.

on the slope (57.8, with a threshold value of 38.6) and a rapid wash-in TIC pattern on DCE-MRI. When we applied the DW-MRI ADC value ( $3.53 \times 10^{-3} \text{ mm}^2/\text{s}$ , with a threshold value of  $1.42 \times 10^{-3} \text{ mm}^2/\text{s}$ ), we correctly modified the diagnosis of the benign cyst. One explanation for the slope of this particular case is that although the cyst may exhibit high microvessel density and abundant blood flow represented by the high slope value and rapid wash-in pattern, the lower cellularity and cysts filled with mucoid or brown fluid that were considered to reflect the ADC value may potentially be larger than the malignant tumor. Therefore, referring to the ADC values is particularly useful when differentiating benign lesions exhibiting an elevated slope value and a malignant TIC pattern.

The DW-MRI findings in this study demonstrated that the mean ADC of malignant tongue tumors was substantially lower than the mean ADC of benign tongue lesions. When the ADC threshold value was set at  $1.43 \times 10^{-3} \text{ mm}^2/\text{s}$ , the specificity, accuracy, and sensitivity were 83.3%, 79.7%, and 74.6%, respectively. Therefore, the DW-MRI and ADC measurements represent a useful method for differentiating benign lesions from malignant tumors of the tongue. These findings are in concordance with prior studies. Shrinivasan *et al.* (21) indicated that malignant lesions exhibited a significantly lower mean ADC compared to benign lesions. In their study, the threshold ADC value of  $1.3 \times 10^{-3} \text{ mm}^2/\text{s}$  was used to distinguish benign from malignant head and neck lesions. Wang *et al.* (22) demonstrated that the mean ADC of malignant lymphomas and carcinoma was significantly lower than that of benign lesions; an ADC value less than  $1.22 \times 10^{-3} \text{ mm}^2/\text{s}$  was used to predict malignancy. DW-MRI has also been utilized to assess metastatic lymph nodes and the grading of malignancies; the mean ADC value of high-grade malignant lymphoma was significantly lower relative

to SCCs (23, 24). Vandecaveye *et al.* (25) suggested that the ADC of malignant lymph nodes was significantly lower than that of benign lymph nodes and used a threshold value of less than  $0.85 \times 10^{-3} \text{ mm}^2/\text{s}$  to distinguish the malignant versus benign status of each lymph node. In contrast, Sumi *et al.* (26, 27) found that the ADC was significantly greater in metastatic lymph nodes than in benign lymphadenopathy. However, central nodal necrosis is one of the characteristic features of metastatic nodes from head and neck cancers, and the high percentage of necrotic metastatic lymph nodes included in this study most likely contributed to the discrepancy.

The ADC values are ultimately dependent on the changes in the diffusion of protons from water. The diffusion of protons from water to tissues is derived from the influx of extracellular water, transfer of protons through the cell membrane, and diffusion of intracellular water. Because water protons in each compartment contribute differently to the diffusion of protons in tissue, the architectural changes in the tissue alter the ADC. Thus, the SI in DW-MRI and derived ADCs vary with the microstructure and pathophysiological status of the tissue. Malignant tumors are characterized by hypercellularity and enlarged nuclei, both of which act to reduce ADCs. Hypercellularity reduces the extracellular matrix and diffusion space of the extracellular compartment (29, 30), and the larger and more angular nuclei decrease the intracellular dimensions, resulting in reduced ADC values. Therefore, the mean ADC values of malignant tumors are significantly lower than those of benign lesions. Exceptions that could lead to a misdiagnosis are ADC values derived from DW-MRI examinations of mucoepidermoid carcinoma and pleomorphic adenoma in which the mobility of protons are anomalous. In our study, the abundant intracellular and extracellular mucoid and endothelial



Combined DCE- and DW-MRI in the diagnosis of the tongue tumors

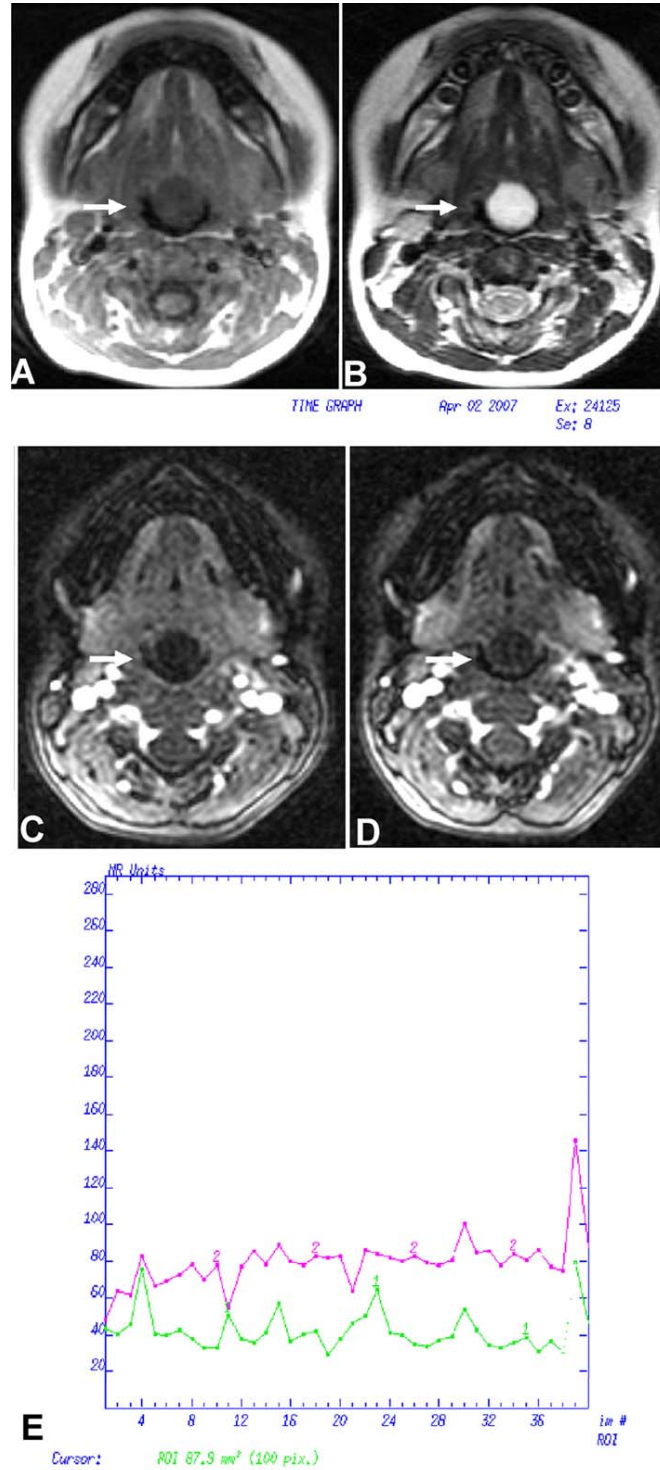


**Figure 6.** Cysts of the tongue root in a 7-year-old boy analyzed by DCE-MRI. (A) Transverse T1-weighted SE MR image shows a hypointense mass (arrowhead) in the tongue root. (B) Transverse T2-weighted FSE MR image shows a homogeneously hyperintense mass (arrowhead). (C) Transverse T1-weighted SE MR image obtained 30 s after contrast material administration shows early enhancement (arrowhead). (D) Transverse T1-weighted SE MR image acquired 228 s after contrast material administration shows completely washed-out patterns (arrowhead). (E) TIC shows an early enhancement peak and a highly washed-out pattern. The slope value is 57.8, which is substantially larger than the threshold value (38.6). When using DCE-MRI or TIC alone, cysts are prone to be diagnosed as malignant. The order of A to E is from left to right.

Combined DCE- and DW-MRI in the diagnosis of the tongue tumors

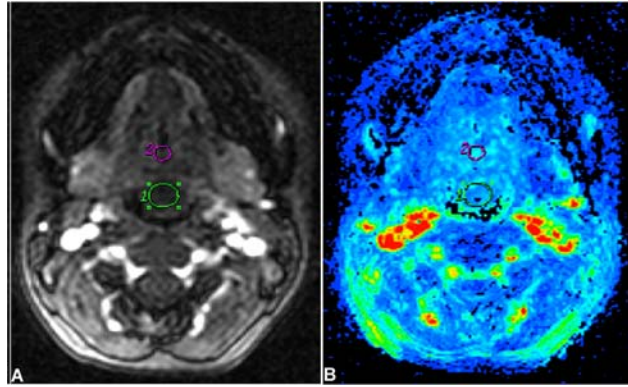


**Figure 7.** Cysts of the tongue root in a 7-year-old boy analyzed by DW-MRI. (A) Transverse DW-MRI image (b-value = 500 s/mm<sup>2</sup>) shows a homogeneously hypointense mass (arrowhead). (B) ADC map shows an extremely low-SE mass. The ADC value is  $3.53 \times 10^{-3}$  mm<sup>2</sup>/s, which is significantly greater than the threshold value ( $1.43 \times 10^{-3}$  mm<sup>2</sup>/s). DW-MRI can lead to an accurate diagnosis of cysts. The order of A to B is from left to right.

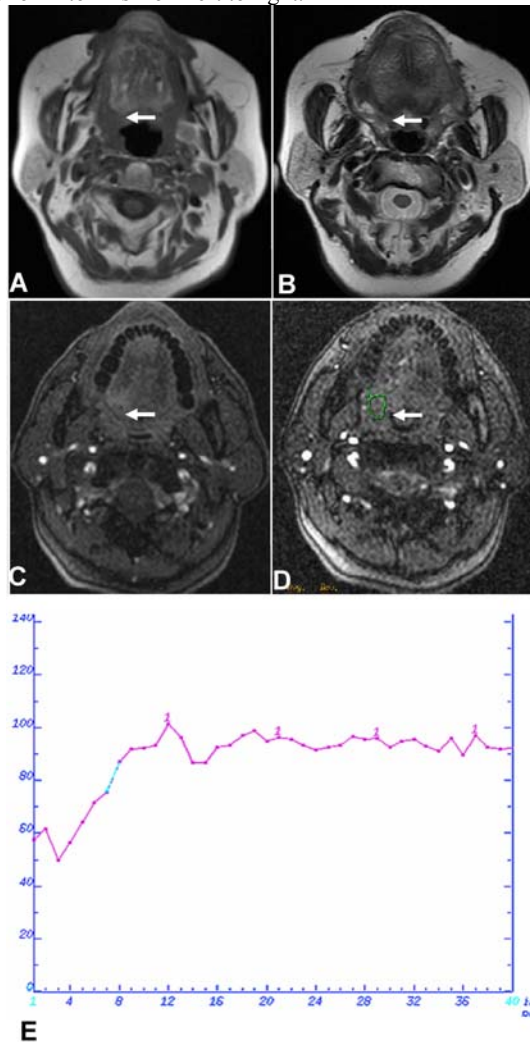


**Figure 8.** Pleomorphic adenoma of the right tongue in a 34-year-old man analyzed by DCE-MRI. (A) Transverse T1-weighted SE MR image shows a hypointense mass (arrowhead) in the right tongue root. (B) Transverse T2-weighted FSE MR image shows a heterogeneously hyperintense mass (arrowhead). (C) Transverse T1-weighted SE MR image obtained 30 s after contrast material administration shows early moderate tumor enhancement. (D) Transverse T1-weighted SE MR image acquired 228 s after contrast material administration shows gradual tumor enhancement. (E) TIC shows a relatively rapid increase in enhancement. The slope value is 35.72, which is lower than the threshold value (38.6). The order of A to E is from left to right.

Combined DCE- and DW-MRI in the diagnosis of the tongue tumors

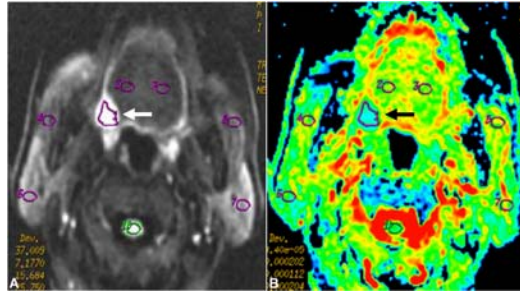


**Figure 9.** Pleomorphic adenoma of the right tongue in a 34-year-old man analyzed by DW-MRI. (A) Transverse DW-MRI image (b-value = 500 s/mm<sup>2</sup>) shows a homogeneously hyperintense mass (arrowhead). (B) ADC map exhibits a high-SI mass. The ADC value is  $1.22 \times 10^{-3}$  mm<sup>2</sup>/s, which is lower than the threshold value ( $1.43 \times 10^{-3}$  mm<sup>2</sup>/s). The order of A to B is from left to right.

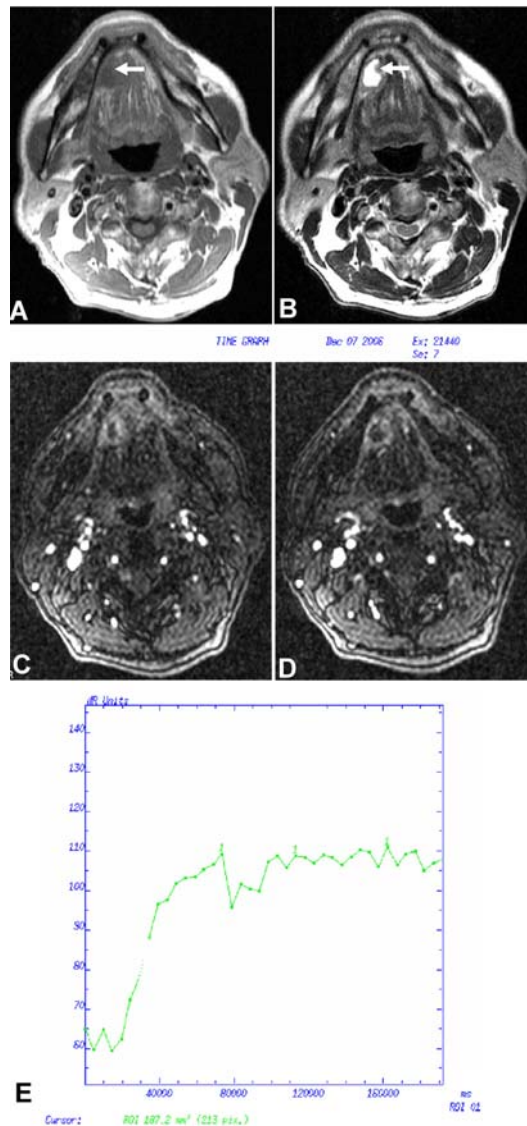


**Figure 10.** Mucoepidermoid carcinoma of the right tongue in a 65-year-old man analyzed by DCE-MRI. (A) Transverse T1-weighted SE MR image shows a hypointense mass (arrowhead) in the right tongue apex. (B) Transverse T2-weighted FSE MR image shows a homogeneously hyperintense mass (arrowhead). (C) Transverse T1-weighted SE MR image obtained 30 s after contrast material administration shows early enhancement. (D) Transverse T1-weighted SE MR image acquired 3 minutes after contrast material administration shows a low wash-out pattern. (E) TIC shows an early peak of enhancement and a persistent plateau. The slope value is 46.29, which is higher than the threshold value (38.6). The order of A to E is from left to right.

**Table 3.** Performance values of ADC and slope for differentiation of benign from malignant tongue tumors

Performance Value	ADC (b=500 s/mm <sup>2</sup> )	Slope
Threshold Value	$1.43 \times 10^{-3} \text{ mm}^2/\text{s}$	38.6
Sensitivity (%)	74.6	80.3
Specificity (%)	83.3	74.5
Accuracy (%)	79.7	77.9
Positive Predictive Value (%)	89.9	89.2
Negative Predictive Value (%)	59.4	60.1

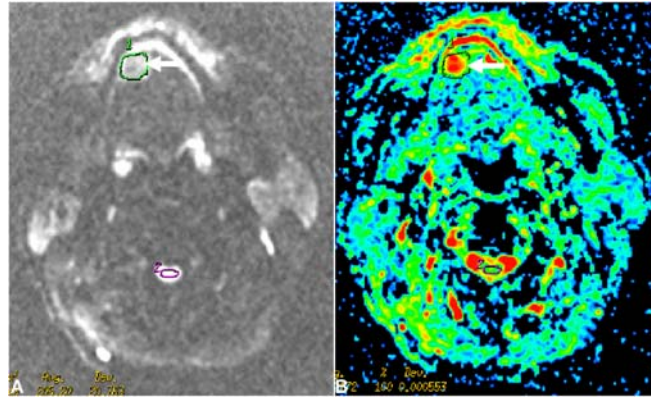


**Figure 11.** Mucoepidermoid carcinoma of the right tongue in a 65-year-old man analyzed by DW-MRI. (A) Transverse DW-MRI image (b-value = 500 s/mm<sup>2</sup>) shows a heterogeneously hyperintense mass (arrowhead). (B) ADC map exhibits a low-SI mass. The ADC value is  $1.72 \times 10^{-3} \text{ mm}^2/\text{s}$ , which is significantly higher than the threshold value ( $1.43 \times 10^{-3} \text{ mm}^2/\text{s}$ ). The order of A to B is from left to right.

proliferation potentially explain the abnormally high ADC value ( $1.72 \times 10^{-3} \text{ mm}^2/\text{s}$ , with a threshold of  $1.43 \times 10^{-3} \text{ mm}^2/\text{s}$ ) exhibited by a malignant mucoepidermoid carcinoma. Additionally, the diffuse high cellularity of glandular cells and fibrosis in the stroma of a pleomorphic adenoma may have potentially disturbed the diffusion of water protons in the extracellular fraction and, therefore, led to the abnormally low ADC value ( $1.22 \times 10^{-3} \text{ mm}^2/\text{s}$ , with a threshold of  $1.43 \times 10^{-3} \text{ mm}^2/\text{s}$ ). The addition of the slope values from DCE-MRI examinations correctly modified the diagnoses obtained from the ADC measurements in cases of mucoepidermoid carcinoma and pleomorphic adenoma (with slopes 46.29 and 35.71, respectively, in which the threshold was 38.6). A reasonable explanation for these modifications is that, although the pleomorphic adenoma exhibited a hypercellularity that mimicked malignancy and the mucoepidermoid carcinoma exhibited the abundant mucoid component normally regarded as a sign of benign tissue, the hemodynamic information represented by the slope obtained from DCE-MRI reflected the appropriate diagnosis. Therefore, the addition of DCE-MRI to DW-MRI might improve the diagnostic accuracy in the characterization of tongue tumors.

This study contains some limitations. We included a relatively small number of benign tongue lesions. A further investigation that includes a larger number of cases is necessary to verify the results of this preliminary study. Yabuuchi *et al.* (16) reported that the addition of DW-MRI to DCE-MRI improved diagnostic accuracy in the characterization of parotid gland tumors. Our study indicates that DW-MRI images improved the accurate diagnosis of a cyst and that the addition of DCE- to DW-

MRI correctly modified the diagnosis of a pleomorphic adenoma and mucoepidermoid carcinoma. However, there is a possibility of a conflict between DCE-MRI and DW-MRI results in the clinical setting. In this scenario, the radiologist should refer to the patient's other pertinent clinicopathologic information. This includes the patient's age, medical history, symptoms, and signs, in addition to the diagnostic MR images. However, the combination of DCE- and DW-MRI is capable of providing comprehensive information on the histopathological alteration of tongue tumors. To our knowledge, this is the first report on the diagnostic value of using combined DW-MRI and DCE-MRI to characterize tongue tumors.

## 6. CONCLUSION

Either DCE- or DW-MRI alone is useful in differentiating benign lesions from malignant tumors of the tongue. The TIC parameters and patterns derived from DCE-MRI correlate well with the hemodynamic status of tumors, whereas cellularity and nuclear contour are the main determinants for the ADC in DW-MRI. The combination of DCE-MRI and DW-MRI is a comprehensive reflection of the pathological state of the tongue tumor and improves the diagnostic accuracy in differentiating benign lesions from malignant tumors in tongue.

## 7. ACKNOWLEDGEMENTS

I am also pleased to acknowledge the important participation of Wenjing Zhu, and especially to Kerong DAI for assisting in the revise and submission of this manuscript.

8. REFERENCE

1. Johnson PL, Eckard DA, Brecheisen MA, Girod DA, Tsue TT: Percutaneous ethanol sclerotherapy of venous malformations of the tongue. *Am J Neuroradiol* 23: 779-782 (2002)
2. Slaba S, Herbreteau D, Jhaveri HS, Casasco A, Aymard A, Houdart E, Aoun N, Riché MC, Enjolras O, Merland JJ: Therapeutic approach to arteriovenous malformations of the tongue. *Eur Radiol* 8: 280-285 (1998)
3. Wang LC, Kronic AL, Medenica MM, Soltani K, Busbey S: Treatment of hemorrhagic lymphatic malformation of the tongue with a pulsed-dye laser. *J Am Acad Dermatol* 52: 1088-1090 (2005)
4. Edwards PC, Lustrin L, Valderrama E: Dermoid cysts of the tongue: report of five cases and review of the literature. *Pediatr Dev Pathol* 6: 531-535 (2003)
5. Friedrich RE, Li L, Knop J, Giese M, Schmelzle R: Pleomorphic adenoma of the salivary glands: analysis of 94 patients. *Anticancer Res* 25: 1703-1705 (2005)
6. Housset M, Baillet F, Dessard-Diana B, Martin D, Miglianico L: A retrospective study of three treatment techniques for T1-T2 base of tongue lesions: surgery plus postoperative radiation, external radiation plus interstitial implantation and external radiation alone. *Int J Radiat Oncol Biol Phys* 13: 511-516 (1987)
7. Huang SF, Kang CJ, Lin CY, Fan KH, Yen TC, Wang HM, Chen IH, Liao CT, Cheng AJ, Chang JT: Neck treatment of patients with early stage oral tongue cancer: comparison between observation, supraomohyoid dissection, and extended dissection. *Cancer* 112: 1066-1075 (2008)
8. Zbären P, Nuyens M, Loosli H, Stauffer E: Diagnostic accuracy of fine-needle aspiration cytology and frozen section in primary parotid carcinoma. *Cancer* 100: 1876-1883 (2004)
9. Som PM, Biller HF: High-grade malignancies of the parotid gland: identification with MR imaging. *Radiology* 173: 823-826, (1989)
10. Freling NJ, Molenaar WM, Vermey A, Mooyaart EL, Panders AK, Annyas AA, Thijn CJ: Malignant parotid tumors: clinical use of MR imaging and histologic correlation. *Radiology* 185: 691-696 (1992)
11. Teresi LM, Lufkin RB, Wortham DG, Abemayor E, Hanafée WN: Parotid masses: MR imaging. *Radiology* 163: 405-409 (1987)
12. Swartz JD, Rothman MI, Marlowe FI, Berger AS: MR imaging of parotid mass lesions: attempts at histopathologic differentiation. *J Comput Assist Tomogr* 13: 789-796 (1989)
13. Yankeelov TE, Gore JC: Dynamic Contrast Enhanced Magnetic Resonance Imaging in Oncology: Theory, Data Acquisition, Analysis, and Examples. *Curr Med Imaging Rev* 3: 91-107 (2009)
14. Asaumi J, Yanagi Y, Konouchi H, Hisatomi M, Matsuzaki H, Kishi K: Application of dynamic contrast-enhanced MRI to differentiate malignant lymphoma from squamous cell carcinoma in the head and neck. *Oral Oncol* 40: 579-584 (2004)
15. Hisatomi M, Asaumi J, Yanagi Y, Unetsubo T, Maki Y, Murakami J, Matsuzaki H, Honda Y, Konouchi H: Diagnostic value of dynamic contrast-enhanced MRI in the salivary gland tumors. *Oral Oncol* 43: 940-947 (2007)
16. Yabuuchi H, Fukuya T, Tajima T, Hachitanda Y, Tomita K, Koga M: Salivary gland tumors: diagnostic value of gadolinium-enhanced dynamic MR imaging with histopathologic correlation. *Radiology* 226: 345-354 (2003)
17. Xian J, Zhang Z, Wang Z, Li J, Yang B, Man F, Chang Q, Zhang Y: Value of MR imaging in the differentiation of benign and malignant orbital tumors in adults. *Eur Radiol* 20: 1692-1702 (2010)
18. Ariyoshi Y, Shimahara M: Relationships between dynamic contrast-enhanced MRI findings and pattern of invasion for tongue carcinoma. *Oncol Rep* 15: 1339-1143 (2006)
19. Le Bihan D, Mangin JF, Poupon C, Clark CA, Pappata S, Molko N, Chabriat H: Diffusion tensor imaging: concepts and applications. *J Magn Reson Imaging* 13: 534-546 (2001)
20. Yabuuchi H, Matsuo Y, Kamitani T, Setoguchi T, Okafuji T, Soeda H, Sakai S, Hatakenaka M, Nakashima T, Oda Y, Honda H: Parotid gland tumors: can addition of diffusion-weighted MR imaging to dynamic contrast-enhanced MR imaging improve diagnostic accuracy in characterization? *Radiology* 249: 909-916 (2008)
21. Srinivasan A, Dvorak R, Perni K, Rohrer S, Mukherji SK: Differentiation of benign and malignant pathology in the head and neck using 3T apparent diffusion coefficient values: early experience. *Am J Neuroradiol* 29: 40-44 (2008)
22. Wang J, Takashima S, Takayama F, Kawakami S, Saito A, Matsushita T, Momose M, Ishiyama T: Head and neck lesions: characterization with diffusion-weighted echo-planar MR imaging. *Radiology* 220: 621-630 (2001)
23. Maeda M, Kato H, Sakuma H, Maier SE, Takeda K: Usefulness of the apparent diffusion coefficient in line scan diffusion-weighted imaging for distinguishing between squamous cell carcinomas and malignant lymphomas of the head and neck. *Am J Neuroradiol* 26: 1186-1192 (2005)
24. Maeda M, Maier SE, Sakuma H, Ishida M, Takeda K: Apparent diffusion coefficient in malignant lymphoma and carcinoma involving cavernous sinus evaluated by line scan



## Combined DCE- and DW-MRI in the diagnosis of the tongue tumors

diffusion-weighted imaging. *J Magn Reson Imaging* 24: 543-548 (2006)

25. Vandecaveye V, De Keyzer F, Vander Poorten V, Dirix P, Verbeken E, Nuyts S, Hermans R: Head and neck squamous cell carcinoma: value of diffusion-weighted MR imaging for nodal staging. *Radiology* 251:134-146 (2009)

26. Sumi M, Sakihama N, Sumi T, Morikawa M, Uetani M, Kabasawa H, Shigeno K, Hayashi K, Takahashi H, Nakamura T: Discrimination of metastatic cervical lymph nodes with diffusion-weighted MR imaging in patients with head and neck cancer. *Am J Neuroradiol* 24: 1627-1634 (2003)

27. Sumi M, Van Cauteren M, Nakamura T: MR microimaging of benign and malignant nodes in the neck. *AJR Am J Roentgenol* 186: 749-757 (2006)

28. Murakami T, Nakamura H, Tsuda K, Ishida T, Tomoda K, Hori S, Monden M, Kanai T, Wakasa K, Sakurai M: Contrast-enhanced MR imaging of intrahepatic cholangiocarcinoma: pathologic correlation study. *J Magn Reson Imaging* 5: 165-170 (1995)

29. Sugahara T, Korogi Y, Kochi M, Ikushima I, Shigematu Y, Hirai T, Okuda T, Liang L, Ge Y, Komohara Y, Ushio Y, Takahashi M: Usefulness of diffusion-weighted MRI with echo-planar technique in the evaluation of cellularity in gliomas. *J Magn Reson Imaging* 9: 53-60 (1999)

30. Stadnik TW, Chaskis C, Michotte A, Shabana WM, van Rompaey K, Luybaert R, Budinsky L, Jellus V, Osteaux M: Diffusion-weighted MR imaging of intracerebral masses: comparison with conventional MR imaging and histologic findings. *Am J Neuroradiol* 22: 969-976 (2001)

**Abbreviations:** MRI, Magnetic resonance imaging; CT, computed tomography; SCC, Squamous cell carcinoma; MDCT, All Multi detector

**Key Words:** Diffusion; Dynamic; enhancement; MRI, Tongue, Tumor

**Send correspondence to:** Qiang Yu, Department of Radiology, Shanghai Ninth People's Hospital, School of Medicine, Shanghai Jiao Tong University, Shanghai, China, Tel: 86-21-23271699, Fax: 86-21-63136856, E-mail: yuqiang6155@sina.cn